Imaging neuroinflammation: Winkeler and colleagues provide an overview of current methods for imaging neurologic inflammation, with emphasis on radioisotopic techniques. . . . . ***Page 1***

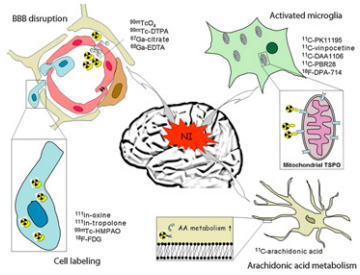

Assessing PET/CT reports: Graham reviews quality and significance factors relative to data generated for the National Oncologic PET Registry and previews an article in this issue of *JNM* on PET/CT reports from this database. . . . . ***Page 5***

PET and dopamine cell transplantation: Ma and colleagues expand on previous work to report on long-term clinical outcomes, including those assessed by ^{18}F-FDOPA PET imaging, in patients with Parkinson disease treated with embryonic dopamine cell implantation. . . . . ***Page 7***

Automated PET/CT amplitude gating: Chang and colleagues present an automated respiratory amplitude gating technique for implementation on current whole-body PET/CT scanners that would obviate breath-holding without increased radiation exposure. . . . . ***Page 16***

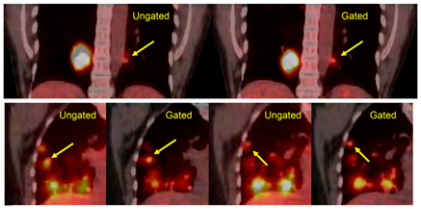

^{18}F-FDG avidity in lymphoma: Weiler-Sagie and colleagues report on the results of ^{18}F-FDG PET/CT in a large cohort of patients newly diagnosed with Hodgkin disease and non-Hodgkin lymphoma, with special attention to tracer avidity in distinct subtypes of lymphoma. . . . . ***Page 25***

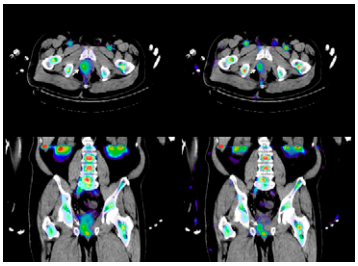

SPECT/CT prostate tumor grading: Seo and colleagues describe phantom studies evaluating a method using ^{111}In-capromab pendetide SPECT/CT for in vivo quantification of antibody uptake and accurate staging of prostate tumors. . . . . ***Page 31***

^{18}F-FMISO in head and neck cancer: Wang and colleagues use pharmacokinetic analysis of ^{18}F-FMISO dynamic PET to delineate regional tumor hypoxia and investigate relationships among various quantifiable and functional factors in patients with head and neck cancer. . . . . ***Page 37***

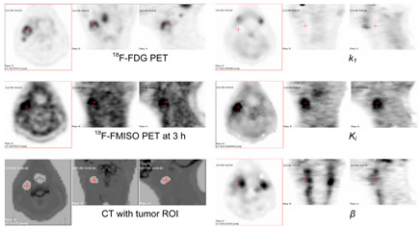

CZT nuclear cardiac imaging: Herzog and colleagues establish optimal scan times for nuclear myocardial perfusion imaging on an ultrafast cardiac γ-camera using novel cadmium-zinc-telluride solid-state detector technology. . . . . ***Page 46***

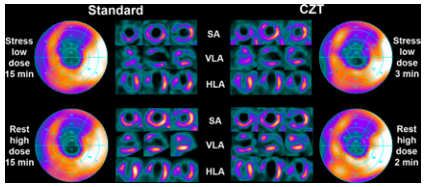

Imaging cirrhotic portal hypertension: Gao and colleagues investigate the diagnostic utility and clinical significance of transsplenic portal scintigraphy in evaluating cirrhotic portal hypertension and compensatory circulation. . . . . ***Page 52***

^{13}N PET in COPD: Vidal Melo and colleagues report on the use of ^{13}N-saline PET for assessment of spatial heterogeneity of lung perfusion as an early biomarker of pulmonary vascular involvement in patients with chronic obstructive pulmonary disease. . . . . ***Page 57***

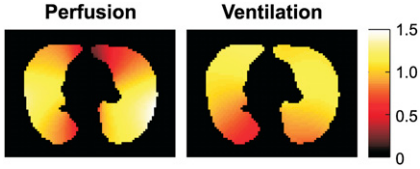

PET in radiotherapy planning: Troost and colleagues provide an educational overview of the current role and future potential of PET for selection and delineation of radiotherapy target volumes and for biologic characterizations of tumor entity. . . . . ***Page 66***

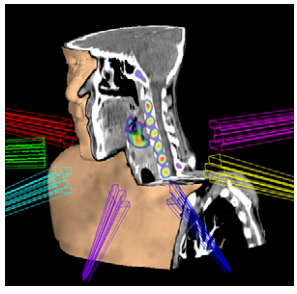

COMKAT software for image quantification: Fang and colleagues describe an integrated, open-source software package with multiple functions for incorporating tracer pharmacokinetic analysis into molecular imaging research. . . . . ***Page 77***

^{64}Cu-C-ANF PET in atherosclerosis: Liu and colleagues explore the potential of a radiolabeled C-type atrial natriuretic peptide factor for vascular targeting in PET imaging of developing atherosclerotic plaquelike lesions. . . . . ***Page 85***

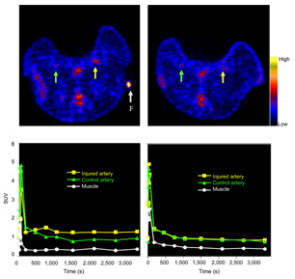

Imaging RAGE: Tekabe and colleagues determine whether expression of the receptor for advanced glycation end products can be detected in atherosclerosis using SPECT and describe the potential for this technique in identifying early accelerated disease in diabetes mellitus. . . . . ***Page 92***

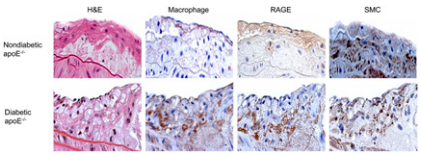

Cancer-targeted multimodal imaging: Hwang and colleagues report on development of and animal studies with an aptamer-conjugated nanoparticle for concurrent in vivo fluorescence, radionuclide, and MR imaging. . . . . ***Page 98***

Genetic PET in breast cancer: Thakur and colleagues investigate the utility of a radiolabeled peptide analog for PET discrimination of breast cancer in a transgenic mouse model and discuss possible applications in early imaging of primary and metastatic disease. . . . . ***Page 106***

PET and cannabinoid receptors: Terry and colleagues evaluate a promising analog with high brain uptake, high specific binding, and reduced uptake in bone for PET imaging of cannabinoid receptors in studies with monkeys and healthy humans. . . . . ***Page 112***

Abl kinase PET: Doubrovin and colleagues assess the feasibility of a PET-based molecular imaging method for direct visualization of Abl kinase expression and protein kinase inhibitor treatment. . . . . ***Page 121***

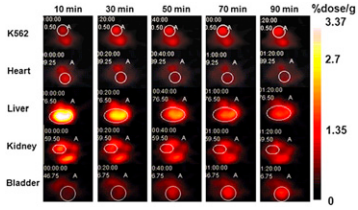

PET and photodynamic therapy: Fei and colleagues explore the use of ^{11}C-choline PET to monitor very early tumor response to photodynamic therapy in mouse models of human prostate cancer. . . . . ***Page 130***

Biodistribution and dosimetry of ^{11}C-(*R*)PK11195: Kumar and colleagues derive biodistribution data and radiation dose estimates for this PET tracer, which facilitates noninvasive imaging of microglial activation in several pediatric and adult neurologic disorders. . . . . ***Page 139***

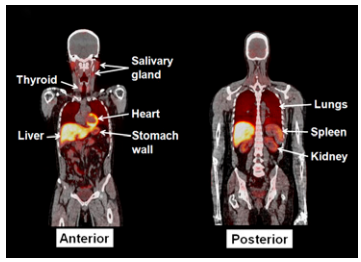

Dosimetry of ^{18}F-PBR06 in humans: Fujimura and colleagues estimate radiation absorbed doses for this PET tracer that measures the translocator protein 18 kDa, a biomarker for inflammation in the human brain. . . . . ***Page 145***

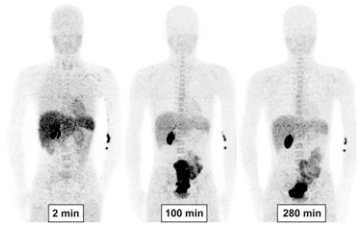

Rituximab and ^{90}Y-ibritumomab dosimetry: Shen and colleagues determine whether the therapeutic effects of ^{90}Y-ibritumomab in relapsed B-cell non-Hodgkin lymphoma might be enhanced by a full course of rituximab followed by single dose of ^{90}Y-ibritumomab. . . . . ***Page 150***

PET and PET/CT reports: Coleman and colleagues use data from the National Oncologic PET Registry database to identify core elements for inclusion in oncologic PET reports and evaluate a sample subset of these reports. . . . . ***Page 158***

ON THE COVER

Clinical benefit and graft viability have been found to be sustained for up to 4 y after transplantation of human embryonic dopaminergic tissue for advanced Parkinson disease. Changes in imaging measures, as shown by these maps of mean striatal ^{18}F-FDOPA uptake in transplant recipients, were associated with clinical outcome over the entire posttransplantation time course.

See page 11.